ON THE USE OF H_α AND HeII 4686 AS MASS-LOSS AND LUMINOSITY INDICATORS FOR HOT STARS

ASTRID GABLER, RUDOLF GABLER, ADALBERT PAULDRACH, JOACHIM PULS, ROLF-PETER KUDRITZKI
Universitätssternwarte München, Scheinerstr.1,
8000 München 80

ABSTRACT By the example of a typical O4 f star like ζ-Puppis, the applicability of H_α and He II 4686 for the determination of mass-loss rates is demonstrated. The comparison of our *"unified model atmosphere"* calculations to earlier work shows that the approximations concerning the atmosphere and the radiation transport made there can lead to large errors, especially in the case of high or low mass-loss rates. Therefore, we propose to use the results of our calculations directly for the mass-loss determination from observed equivalent widths of H_α and He II 4686 - furthermore, because the He II 6560 Blend is taken correctly into account in our profile calculation of H_α, which has an effect of 0.2 dex in the resulting mass-loss rate for ζ-Puppis. The second application of these two lines is to use them as luminosity indicators for Central Stars of Planetary Nebulae (CSPN). Our theoretical calculated profiles show the same behaviour as the observed ones: they switch over from absorption to emission as the stars approach the Eddington limit. Thus the wind lines together with the photospheric lines give us a *purely spectroscopic method* for the determination of L,M,R,T_{eff} and distances at hand.

INTRODUCTION

The determination of accurate mass-loss rates is one of challenging problems in hot star spectroscopy. Originally, after the advent of the UV-sensitive rocket and satellite telescopes, the P-Cygni type profiles of UV resonance lines were used to determine the terminal wind velocity $\mathbf{v_\infty}$ and the mass-loss rate $\dot{\mathbf{M}}$. However, it soon became clear that the rates determined in this way depend crucially on the way how the ionisation in the wind is calculated. Therefore, the alternative and more accurate method to use radio observations of the thermal emission from hot stars became more important. However, because of the sensitivity of present day radio telescopes, this method is limited to the brightest objects only. On

the other hand, winds of hot stars produce also line emission in H_α and He II 4686, which in principle can also be used to determine mass-loss rates. The great advantage of such a method is the applicability even for very faint objects in distant galaxies and its independence from the knowledge of the metallicity of the observed stars.

Another interesting application is the case of the Central Stars of PN (CSPN). These objects show also winds depending in strength on stellar mass and luminosity. We will demonstrate that this provides us with a new method to determine directly stellar luminosities.

H_α AND He II 4686 AS MASS-LOSS INDICATORS

FORMER WORK

Several steps in this direction were already done earlier by Klein and Castor (1978), Olson and Ebbets (1981), Cassinelli et. al. (1978) and recently by Leitherer (1988). H_α wind emission was calculated by means of NLTE/Sobolev methods what showed undoubtedly that the winds around hot stars provide enough emission measure to explain qualitatively the observed H_α emission profiles. Quantitatively, however, these calculations are insufficient because of two reasons:

- First, they divide the atmosphere artificially and ad hoc in two separate regions: a hydrostatic, photospheric part and the supersonic wind region. The borderline between these two regions is defined by the free parameters radius r_0 and either velocity v_0 or density ρ_0. Unfortunately, as test calculations not only for H_α and He II 4686 but also for the near and far IR make evident, the calculations depend crucially on these parameters.

- Second, the radiative interaction between these two regions is treated in a very simplified way: Only the wind emission additionally to a photospheric continuum is calculated. However, part of the H_α profile, e.g. the Stark-broadened wings, is formed in the photosphere and H_α is a complicated mixture of photospheric and wind photons. Sometimes, this is approximated by the very simple procedure of only adding the flux line-profiles of hydrostatic, plane-parallel models and wind emission to give the final emergent profile.

It is clear that this is a very limited procedure - but we have to check if it's accuracy is still sufficient compared to the inaccuracies involved in UV-work.

UNIFIED MODEL ATMOSPHERES

We use our *"unified model atmosphere code"* to calculate correct theoretical H_α profiles, which avoids the artificial division between photosphere and wind (for all details see the contribution by R. Gabler et.al., this meeting, or R.Gabler et.al., 1989).

In the final formal integral to calculate the emergent H_α and He II 4686 profiles *Stark-broadening* is taken into account in addition to the effects of the velocity field. Vidal-Cooper-Smith theory is applicated for H_α whereas for He II 4686 the broadening tables from Schöning and Butler (1989) are used. As we have found, the inclusion of Stark-broadening is crucial for quantitative fits.

Normally, T_{eff}, log g and the stellar radius R are the only free parameters in our models, because they also define the radiative line force and its parameters **k, α, δ** and yield finally v(r) and $\dot{M}$. In this case, however, we give up the full selfconsistency and use k and α as free parameters to produce a sequence of models with different $\dot{M}$ but constant v_∞ (δ has been set equal to zero for simplicity). Table I summarizes the values choosen for our example - a typical O4f star with T_{eff} = 45 000 K, log g = 3.6, $R/R_\odot$ = 18.

TABLE I

model	k	α	v_∞(km·s^{-1})	$\dot{M}$($10^{-6}\cdot M_\odot\cdot yr^{-1}$)	log $\dot{M}$
1	.0001	.70	2376	.0006	- 9.22
2	.001	.69	2340	.0136	- 7.87
3	.01	.68	2287	.3358	- 6.47
4	.02	.68	2311	.9240	- 6.03
5	.05	.68	2338	3.523	- 5.45
6	.07	.68	2353	5.760	- 5.24
7	.1	.68	2363	9.690	- 5.01
8	.2	.675	2329	26.11	- 4.58
9	.3	.675	2352	47.39	- 4.32
10	.5	.675	2368	100.4	- 4.00

The resulting density structure for some of these models is given in Figure 1. As enhancing the mass-loss rate, the sonic point moves further into the atmosphere.

The corresponding sequence of H_α- profiles is shown in Figure 2. The sensitivity of H_α with respect to the mass-loss rate is obvious. The profile turns over from a pure absorption profile to a broad emission feature when the mass-loss rate is enhanced.

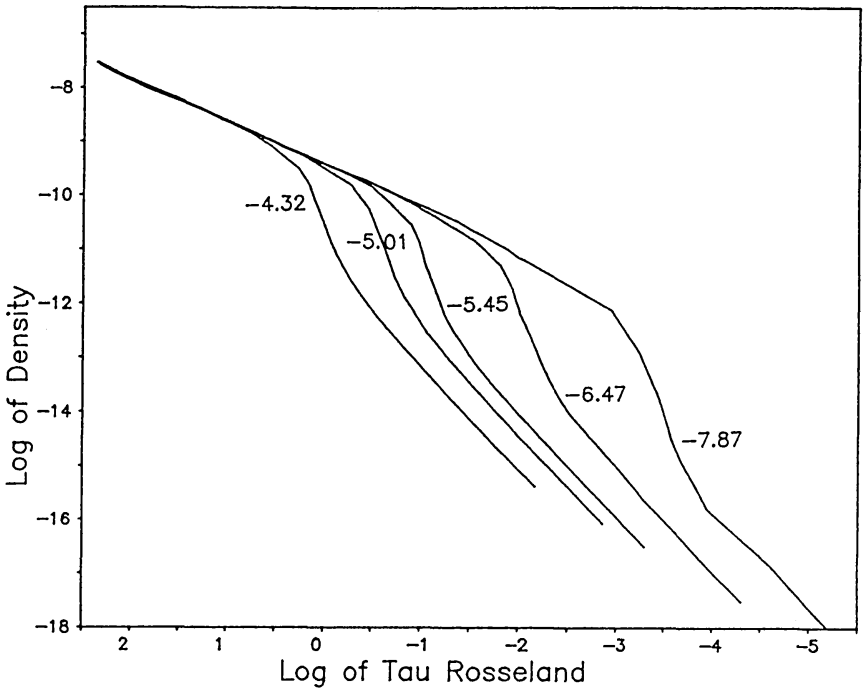

Fig. 1 log $\rho(r)$ versus log τ_{Ross} for some of the models from Table I. Log $\dot{M}$ is indicated at each curve.

To compare with the approximate procedure (for details see Leitherer, 1988) we proceed as follows:
We define the *emission equivalent width* of H_α:

$$W_\lambda(H_\alpha) = \int_{-\infty}^{\infty} \left(\frac{H_{\Delta\lambda}}{H_{cont}} - 1 \right) d(\Delta\lambda) \qquad (2)$$

Leitherer (1988) shows, that in the approximate procedure the *observed equivalent width* of H_α is related to the mass-loss rate and stellar parameters by:

$$\log \left[\left(W_\lambda(H_\alpha) + W_\lambda^{Phot}(H_\alpha) \right) \cdot L_\lambda(H_\alpha) \right] =$$

$$2 \log \dot{M} - 2 \log v_\infty - \log R/R_\odot + C(T_{eff}) + 25.125 + I \qquad (3)$$

$L_\lambda(H_\alpha)$ is the continuous spectral luminosity close to H_α, W_λ (H_α) the absorption equivalent width of the corresponding hydrostatic, photospheric NLTE-model. Taking the parameters of our example, equation (3) reduces to:

$$\log \dot{M} = 0.5 \cdot \left(\log \left(W_\lambda(H_\alpha) + W_\lambda^{Phot}(H_\alpha) \right) - 11.271 \right) \qquad (4)$$

This approximate relation is shown in Figure 3 in comparison to

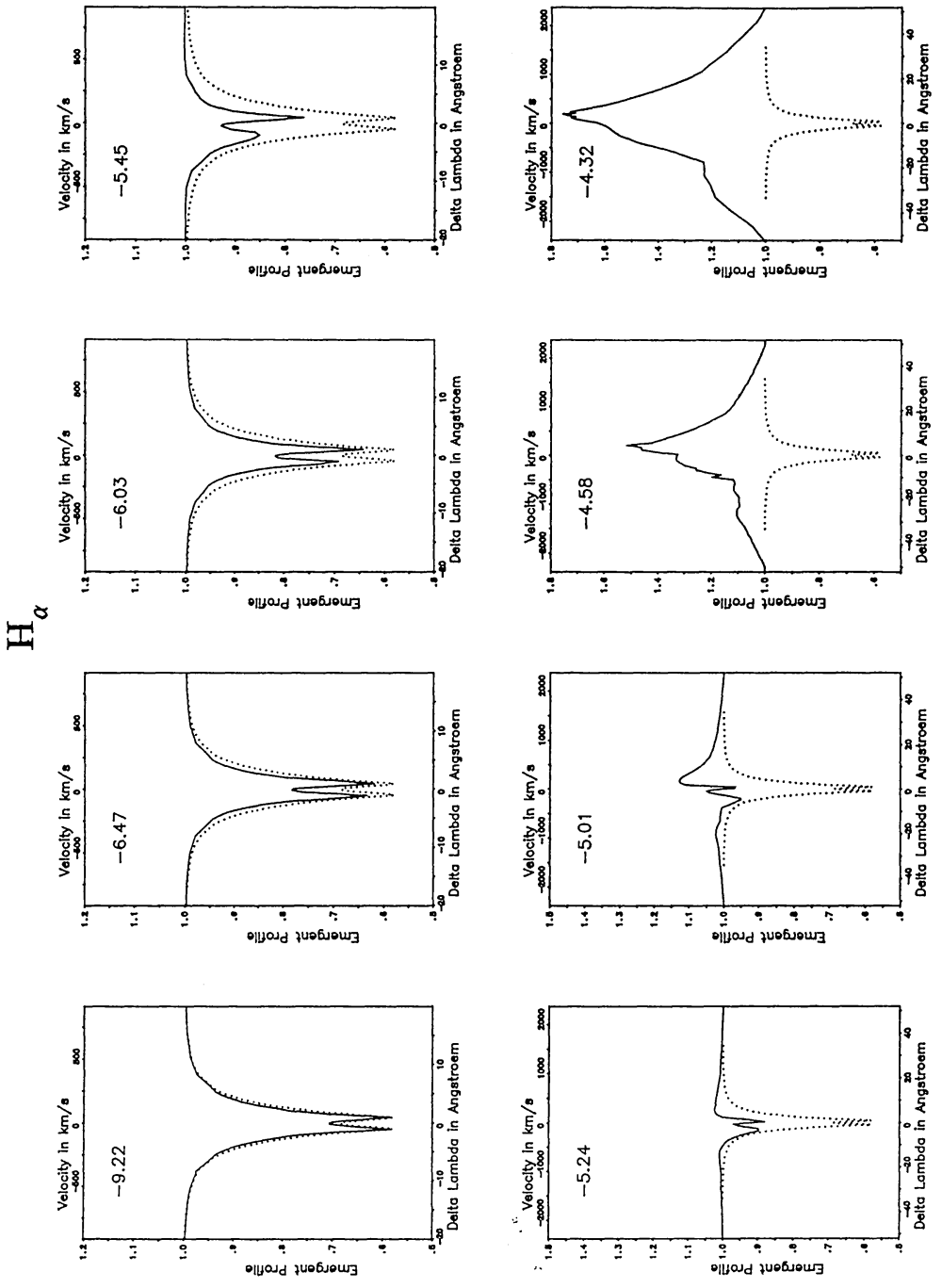

Fig. 2 The sequence of theoretical calculated Hα profiles (solid curve) in comparison to the profile from a plane-parallel, hydrostatic model (dotted).

the results of our unified models.

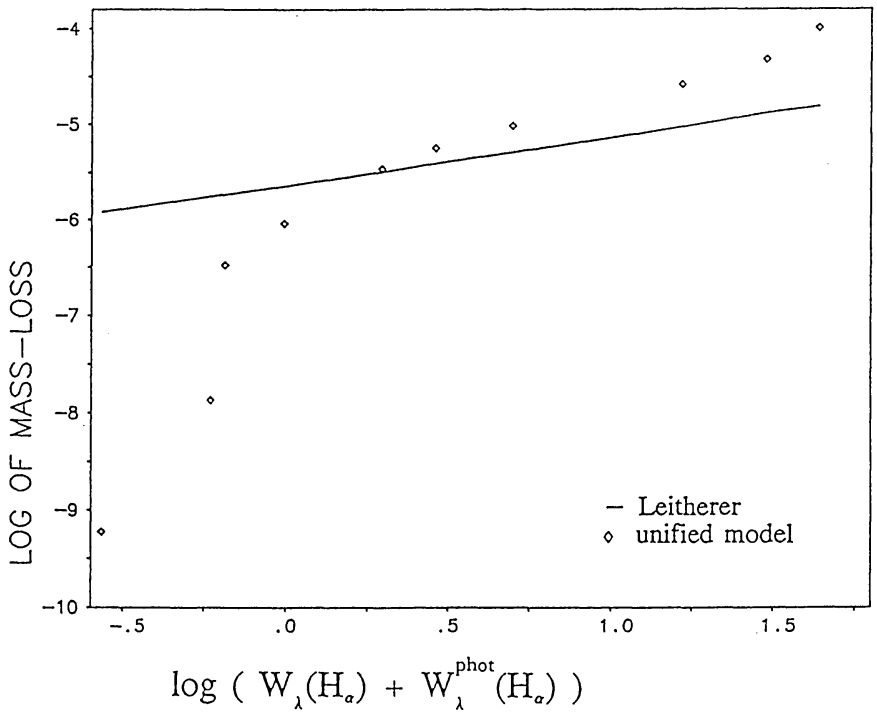

Fig. 3 log $\dot{M}$ as function of $W_\lambda(H_\alpha) + W_\lambda^{Phot}(H_\alpha)$. The approximate equation (4) (solid curve) is shown in comparison to the results of our unified models (dotted).

In the relevant domain between $-6.0 < \log \dot{M} < -5.0$ the approximate procedure is sufficient within a factor of two. For higher or smaller mass-loss rates $\dot{M}$ it fails significantly. The reasons for this failure are obvious:

For high mass-loss rates $\dot{M}$, the assumption of optical thin H_α ($\tau_{H\alpha} \ll 1$) made in the derivation of equation (3) no longer holds in this case of a very dense stellar wind.

In the case of low $\dot{M}$, H_α is nearly "photospheric" and the artificial division between wind and photosphere leads to crucial errors.

A great disadvantage of the approximate procedure is the use of the spurious *"photospheric"* H_α equivalent width, which is physically unrealistic, not well defined and introduces additional errors, which may become significant.

We, therefore, propose to use our theoretical calculated equivalent width directly for the determination of mass-loss rates. Figure 4 allows one to read off log $\dot{M}$ directly as $W_\lambda(H_\alpha)$ is observed.

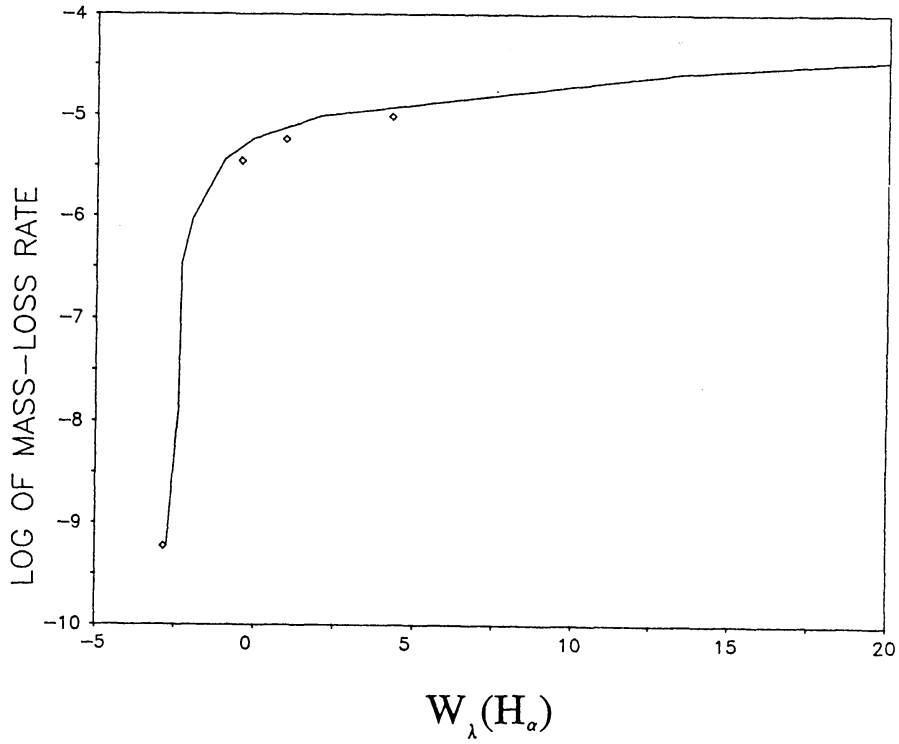

Fig. 4 Log $\dot{M}$ against the equivalent width $W_\lambda(H_\alpha)$. Calculations without HeII 6560 blend (solid curve) and new calculations with blend (dots) are shown.

Another very important fact, which was absolutely ignored in all the work up to now, is that the observed H_α profile is always influenced by the nearby blend of HeII 6560. In our calculations it is easy to take this HeII blend correctly into account as additional opacity/emissivity in the formal integral of the source function.

If we want to determine log $\dot{M}$ from Figure 4, using the observed equivalent width for ζ-Puppis which is given as $W_\lambda(H_\alpha)$ = 1.99 (S.Voels, 1989), we get from the old calculations: log $\dot{M}$ = - 5.0. This value is about 0.2 to 0.4 dex too high compared with radio rates. From the calculations with HeII 6560 Blend we get: log $\dot{M}$ = - 5.2, which is much closer to the radio rate, but may be still a bit too high.

The HeII 4686 line allows a similiar procedure as H_α. This line is also very sensitive to the mass-loss rate $\dot{M}$ as is demonstrated in Figure 5 for our example. The theoretical calculated equivalent widths for our example are shown in Figure 6, from which it is possible to read off log $\dot{M}$ for an observed value of W_λ(HeII 4686).

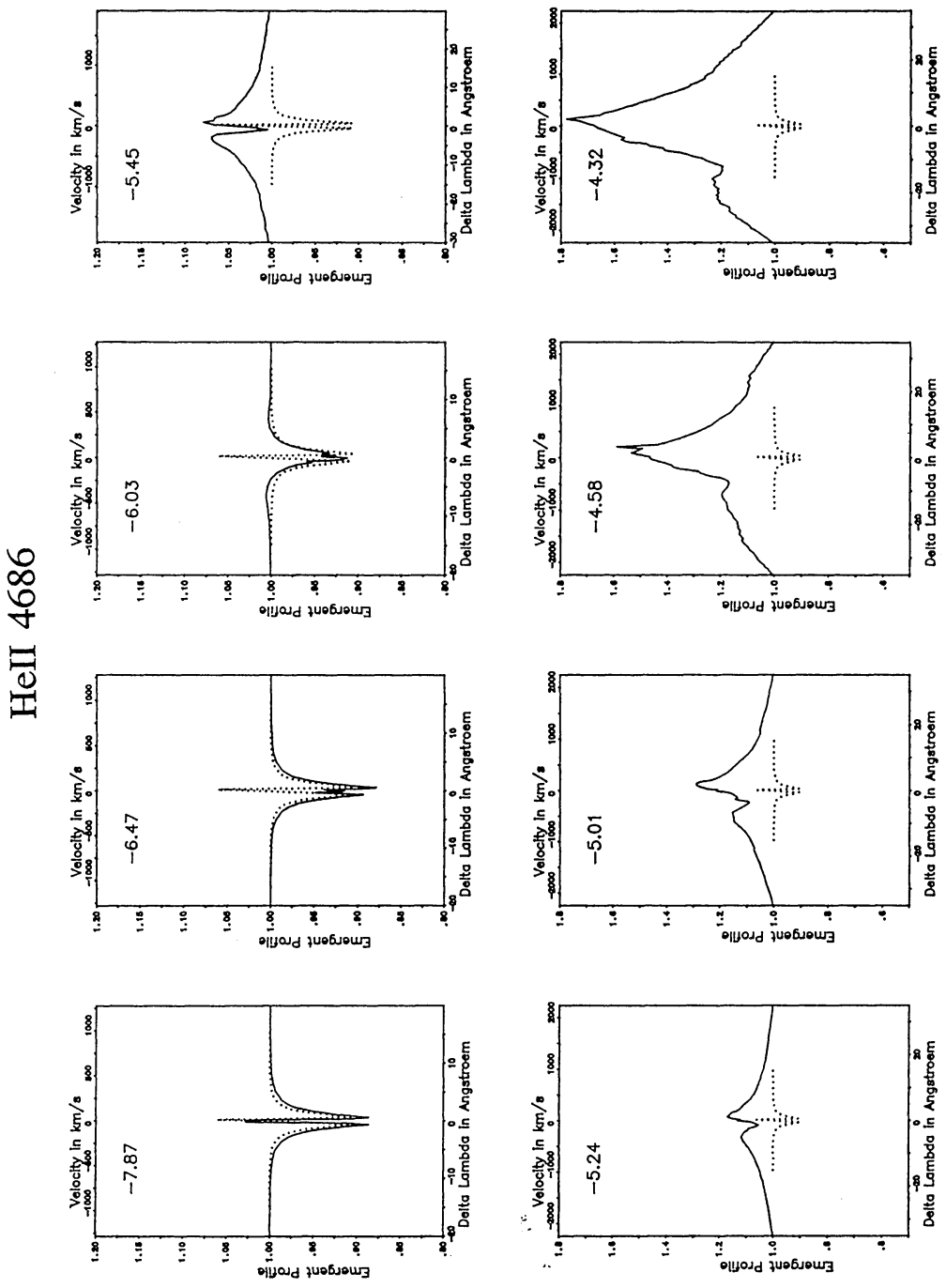

Fig. 5 The sequence of He II 4686 profiles from our unified model calculations (solid curve) in comparison to a profile from a plane-parallel hydrostatic model calculation (dotted).

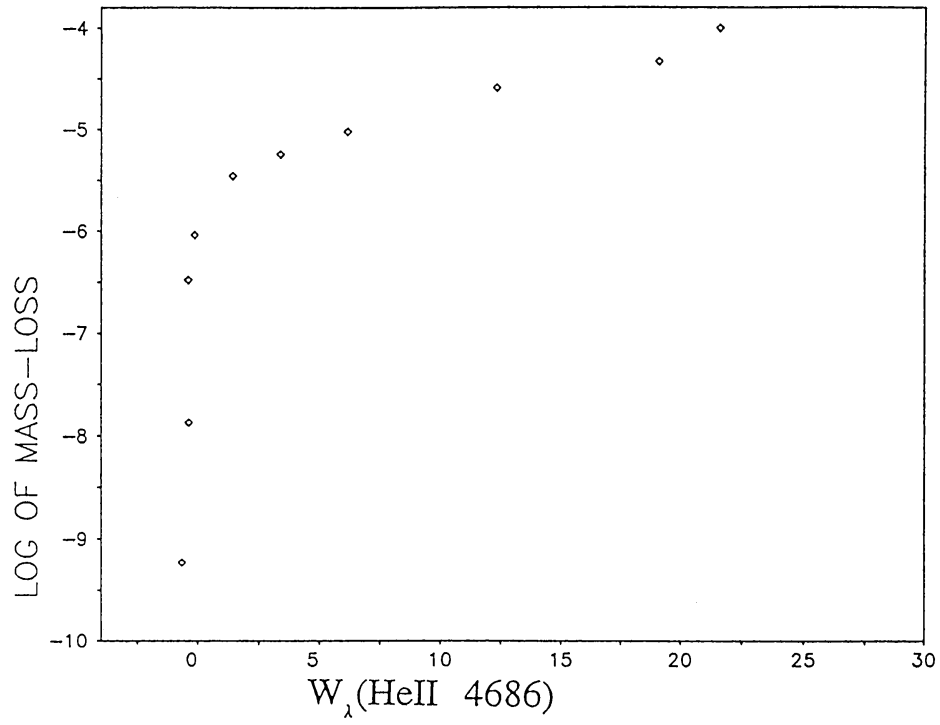

Fig. 6 Log $\dot{M}$ versus the equivalent width W_λ(He II 4686).

For ζ-Pup we observe W_λ(HeII 4686) = 2.12 (S.Voels, 1989), which yields log $\dot{M}$ = - 5.4, which is quite in the right domain compared to radio rates.

As next future steps we want to apply the H_α and HeII 4686 mass-loss determination method on the full HRD domain - for O,B,A-supergiants and luminous blue variables. Another interesting point would be to look after the variability of H_α, which reflects the variability of $\dot{M}$.

HeII 4686 AND H_α AS LUMINOSITY INDICATORS FOR CSPN

Central stars close to the Eddington limit show stellar winds. The following (log g,log T_{eff})-diagram (Figure 7) is obtained by detailed NLTE analysis of photospheric lines done by R.Mėndez et. al. (1988). Evolutionary tracks, labelled by the stellar mass, are also shown. As demonstrated by A.Pauldrach et. al. (1988), the improved theory of radiation driven winds is appropriate for CSPN. We now have calculated a sequence of models for central stars with T_{eff} = 50 000 K and different stellar masses ranging from 0.55 to 1.0 $M_\odot$. More detailed information about each model is given in Table II.

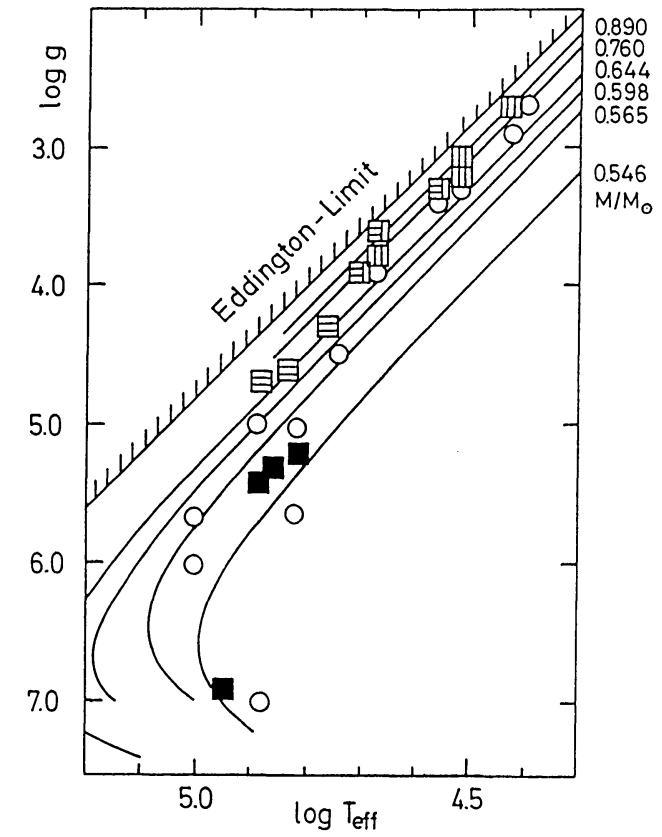

▤ IUE wind detections
▤ wind detections by optical spectra
■ objects with definitely no wind
○ objects with no wind in the optical – but no IUE high resolution information available

Fig. 7 The (log g, log T_{eff})-diagram of the CSPN analysed by Mèndez et.al. (1988). Evolutionary tracks, labelled by the mass are also shown.

TABLE II

$M/M_\odot$	$R/R_\odot$	log g	$\dot{M}(M_\odot\,yr^{-1})$	$v_\infty(km\cdot s^{-1})$	L/L_E
0.55	0.59	4.63	$2.86\cdot10^{-9}$	1658	0.09
0.64	1.24	4.06	$3.84\cdot10^{-8}$	866	0.35
0.75	1.62	3.89	$1.08\cdot10^{-7}$	635	0.52
0.85	1.90	3.81	$2.05\cdot10^{-7}$	520	0.62
1.0	2.24	3.74	$1.33\cdot10^{-6}$	426	0.74

As increasing the mass, the stars come closer to the Eddington limit (see last coulumn of Table II). The resulting HeII 4686 and H_α line profiles are given in Figures 8 and 9. As it is observed, the HeII 4686 line switches over from absorption to emission when the stars approach the Eddington limit - the same is true for H_α. The model with one solar mass is very close to the observed stellar

parameters of NGC 2392 (acc. to Mendez, 1988: T_{eff} = 47 000 K, log g = 3.6, $M/M_{\odot}$ = 0.9) and shows a very strong HeII 4686 emission profile.

To summarize, the improved theory of radiative driven winds together with the spherical extended model atmosphere code gives us a *"purely spectroscopic method"* for the determination of L,M,R,T_{eff} and distances at hand. While we can get T_{eff}, log g and the ratio N(He)/N(H) from the analysis of photospheric spectra, the emission/absorption characteristics of the wind lines He II 4686 (and H_{α}) in the spectra of CSPN can be used to determine stellar mass M and radius R.

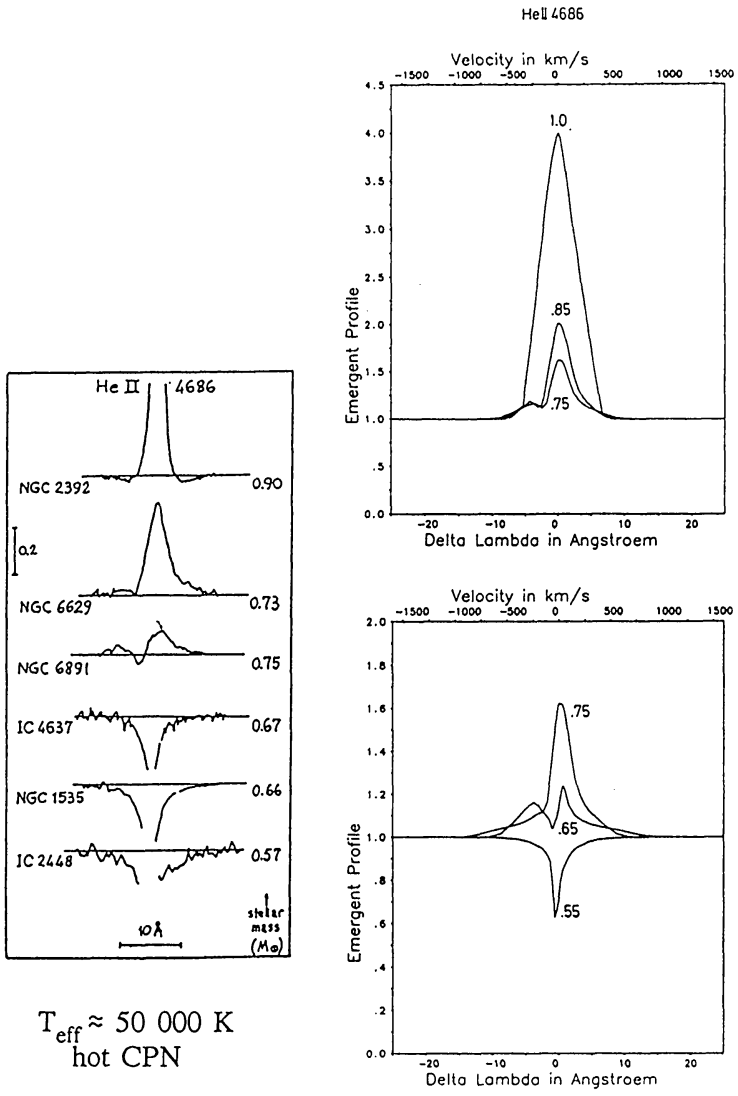

Fig. 8 The observed HeII 4686 line features for hot CSPN ($T_{eff} \approx$50 000 K) beside the results of our theoretical calculated profiles. $M/M_{\odot}$ is indicated at each profile.

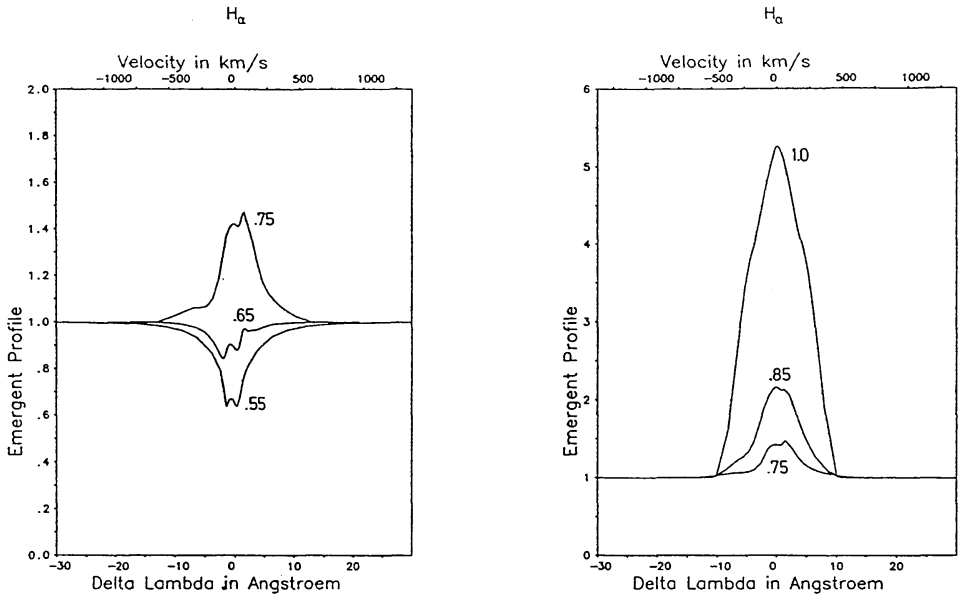

Fig. 9 Theoretical calculated H_α profiles for the models in Table II. The mass in units of $M_\odot$ is indicated at each profile.

ACKNOWLEDGEMENTS

This work was supported within the DFG-Schwerpunkt "Theorie kosmischer Plasmen" under grants Ku 474-11/2 and Ku 474-13/1/2. A travel grant from IBM, Munich to Astrid Gabler is gratefully acknowledged.

REFERENCES

Cassinelli, J.P., Olson ,G.L., Stalio, R. 1978, Ap.J., **220**, 537.
Gabler, R., Gabler, A., Kudritzki, R.P., Puls, J., Pauldrach, A. 1989, Astron. Astrophys., *in press.*
Klein, R.J., Castor, J.I. 1978, Ap.J., **220**, 902.
Leitherer, C. 1988, Ap.J., **326**, 356.
Mėndez, R.H., Kudritzki, R.P., Herrero, A., Husfeld, D., Groth, H.G. 1988, Astron. Astrophys., **190**, 113.
Olson, G.L., Ebbets, D. 1981, Ap.J., **248**, 1021.
Pauldrach, A., Puls, J,, Kudritzki, R.P. 1986, Astron.Astrophys., **164**, 86.
Pauldrach, A., Puls, J., Kudritzki, R.P., Mėndez, R.H. and Heap, S.R. 1988, Astron.Astrophys., **207**, 123.
Schöning, T., Butler, K. 1989a, Astron.Astrophys., **219**, 326.
Schöning, T., Butler, K. 1989b, Astron.Astrophys., **78**, 51.
Vidal, C.R., Cooper, J., Smith, E.W. 1973, Ap.J. Suppl., **25**, 37.
Voels, S. 1989, private communication.